Proceedings of IDETC/CIE 2005
ASME 2005 International Design Engineering Technical Conferences
& Computers and Information in Engineering Conference
September 24-28, 2005, Long Beach, California USA

DETC2005-85693

VIBRATION CONTROL BASED ON A PROBABILISTIC NONLINEAR PROCESSING OF THE PIEZOELEMENT OUTPUT VOLTAGE

Daniel Guyomar
INSA – LGEF
69621 Villeurbanne Cedex
France
daniel.guyomar@insa-lyon.fr

Adrien Badel
INSA – LGEF
69621 Villeurbanne Cedex
France
adrien.badel@insa-lyon.fr

Claude Richard
INSA – LGEF
69621 Villeurbanne Cedex
France
Claude.richard@insa-lyon.fr

Elie Lefeuvre
INSA – LGEF
69621 Villeurbanne Cedex
France
elie.lefeuvre@insa-lyon.fr

ABSTRACT

This paper deals with the so-called SSDI technique which is a semi-passive approach developed to address the problem of structural vibration damping. This technique takes advantage of an original non-linear processing of the voltage generated by piezoelements. It was shown that the original control law corresponding to the SSDI technique was optimal in the case of mono-modal solicitations. In the case of wide band multi-modal solicitation it is not ever true. This paper proposes a novel multi-modal control law for the SSDI technique. It is based on a probabilistic description of the piezovoltage and results in an optimization of the energy dissipated in the nonlinear device connected to the piezoelectric elements.

INTRODUCTION

The problem of structural vibration damping in many industrial sectors such as automobile, aerospace, sport equipment, measurement devices, etc, has instigated a sharp increase in research in the area of vibration control. In this field, piezoelectric materials are of main interest because they are solid state, reliable, lightweight, possess relatively high bandwidths, and consume relatively small amounts of power. These properties are ideal for operating the materials as sensors, actuators or both sensor and actuator. Piezoelectric materials are embedded in the vibrating structure. When the structure vibrates, the piezoelectric elements are stressed and convert part of the mechanical energy by piezoelectric effect. Degradation or transfer of this energy results in control and reduction of the vibration. For active vibration control, a complex system built with at least a sensor, a control unit and a feedback actuator is necessary. In addition, external power sources and amplifier are needed for the control unit and the actuators. The passive techniques can be more easily integrated due to their simplicity and their compactness. The piezoelectric elements are connected to a specific electrical network consisting of a dissipative shunt [1]. The most effective method is the tuned shunt where a circuit made with an inductor and a resistor in series is connected to the capacitance of the piezo-elements. Optimal damping is obtained by tuning the electrical resonance on the frequency of the wanted structural mode. This method leads to good results but has the few following disadvantages: For low frequency modes, the optimal value of the inductor is very large and requires active circuitry. Moreover it is sensible to environmental factors such as temperature, acoustic load, which cause drifts of the structure resonance frequencies. Once detuned, the shunt circuit looses its damping performance. Finally, mutimodal damping requires the use of complex shunt circuits [2].

To bypass these drawbacks, several semi passive or active-passive techniques had been proposed. In the solid-state tunable piezoelectric absorber developed by C. L. Davis and G. A. Lesieutre [3], a passive capacitive shunt circuit is used to electrically adjust the piezoelements effective stiffness and then tune the device resonance frequency. In the approach proposed by R A. Morgan and K. W. Wang [4], an adaptive inductor tuning, a negative resistance and a coupling enhancement set up lead to system with multimodal damping ability.

More recently, switched shunt techniques have been developed introducing a nonlinear approach by using a modulation of the piezoelement properties or boundary

conditions synchronously with the structure motion. They are also based on a discontinuous dissipation or transfer of the mechanical energy. The state switching method proposed by W W Clark [5] is a variable stiffness technique in which piezoelements are periodically held in the open circuit state then switched and held in the short-circuit state, synchronously with the structure motion.

This paper deals with a particular non linear technique which is known as SSDI for Synchronized Switch Damping on Inductor [6, 7, 8]. It consists in a nonlinear processing of the voltage on piezoelectric elements bonded on the structure. It is implemented with a simple switch driven during short periods synchronously with the structure motion. It was shown that the original control law governing this technique was not optimal in the case of wide band multi-modal solicitation. L. R. Corr and W. W. Clark proposed a multi-modal approach which consists in selecting the modes to be controlled and insuring a negative rate of energy change in the selected modes of the structure [8]. The new control law proposed in this paper is based on the idea of maximising the energy dissipated in the nonlinear processing device connected to the piezoelectric elements. It is derived from a probabilistic description of the piezovoltage.

A multi-modal modeling of a clamped free beam with piezoelectric elements is presented in section II. It is based on the model developed by Sodano et al to address piezoelectric energy harvesting problem [10]. The proposed control laws is detailed in section III. Simulations results are given and discussed in section IV.

I. MODELING

It is considered a typical vibrating beam damped by the action of piezoelectric elements, as shown in Fig. 1. The beam is clamped at one end in a rigid structure and piezoelectric inserts are bonded on its surface close to the clamped end where the bending radius is a minimum. In the considered case, the piezoelectric elements are massive ceramics whose poling directions are perpendicular to the beam. It is then the lateral coupling k_{31} which mainly drives the piezoelectric response. This approach can although be generalized to composite piezoelectric inserts where the poling direction may be horizontal. The two piezoelectric elements are electrically connected in parallel. The ground is set to the electrical potential on the piezoelectric elements surfaces in contact with the beam. The characteristics of the beam and of the piezoelectric elements are summarized in Table 1.

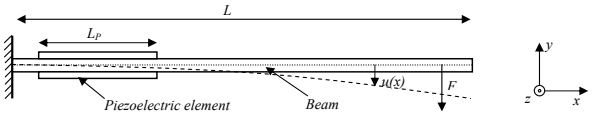

Fig. 1: Vibrating beam with piezoelectric elements

Table 1: Structure characteristics

Structure width	b
Beam length	L
Beam volume	V_B
Beam density	ρ_B
Beam rigidity	c_B
Piezoelements length	L_p
Piezoelements thickness	e_p
Piezoelements volume	V_P
Piezoelements density	ρ_B
Short-circuit piezoelements rigidity	c_P^E
Open-circuit piezoelements rigidity	c_P^D
Piezoelements clamped permittivity	ε^S
Piezoelectric coefficient	e

It is assumed that the structure acts as pure Euler-Bernoulli beam, the stress T and the strain S in the structure are then longitudinal (along the x axis). The electric field E is purely along the y axis, as well as the electrical displacement D. The piezoelectric constitutive equations are then given by (1), where c_P^E is the longitudinal elastic rigidity of the piezoelements when they are short-circuited, ε^S is their clamped permittivity and e the piezoelectric coefficient. In the beam, the relationship between stress and strain is given by (2), where c_B is the longitudinal elastic rigidity of the beam.

$$\begin{bmatrix} T_x \\ D_y \end{bmatrix} = \begin{bmatrix} c_P^E & -e \\ e & \varepsilon^S \end{bmatrix} \begin{bmatrix} S_x \\ E_y \end{bmatrix} \quad (1)$$

$$T_x = c_B S_x \quad (2)$$

In order to give a simple multi-modal lumped model for the cantilever beam with piezoelectric elements, some assumptions must be made. The first assumption follows the Rayleigh-Ritz procedure, which says that the displacement of the beam can be written as the summation of modes in the beam and a temporal coordinate. This is shown in (3), where $\phi_j(x)$ is the mode shapes of the structure, $r_j(t)$ the corresponding temporal coordinate and N the number of mode included in the analysis. The mode shape determination can be done assuming that the structure is homogeneous along the x axis and using typical analytical mode shape for Euler-

Bernoulli beams, or using FEM software. The second assumption is the Euler-Bernoulli one, which allows the strain in the structure to be the product of the distance from the neural axis and the second spatial derivative of the displacement along the beam, which is summarized in (4). The last assumption is that the electric field along the thickness of the piezoelements is constant and linked to the piezovoltage V by (5).

$$u(x,t) = \sum_{j=1}^{N} \phi_j(x) r_j(t) \quad (3)$$

$$S_x = -yu''(x,t) = -y\sum_{j=1}^{N} \phi_j''(x) r_j(t) \quad (4)$$

$$\begin{cases} E_y = -\dfrac{V}{e_p} & \text{for } y > 0 \\ E_y = \dfrac{V}{e_p} & \text{for } y < 0 \end{cases} \quad (5)$$

It is considered that the structure is driven by a punctual force F, at the axis x_F. Using previous assumptions, it was shown 10 that the constitutive equations of the system, governing the displacement of the structure and its electrical behavior can be expressed by (6) and (7). The different parameters and variable of these equations are detailed in Table 2 and Table 3 respectively.

$\forall j = 1...N$

$$\left(M_{Sj} + M_{Pj}\right)\ddot{r}_j + \left(K_{Sj} + K_{Pj}^E\right)r_j + C_j\dot{r}_j - \alpha_j V = \beta_j F \quad (6)$$

$$I = \sum_{j=1}^{N} \alpha_j \dot{r}_j - C_0 \dot{V} \quad (7)$$

Table 2: Parameters of the model

Main parameters	
j[th] beam dynamic mass	$M_{Bj} = \rho_B \int_{V_B} \phi_j(x)^2 \, dV_B$
j[th] piezoelements dynamic mass	$M_{Pj} = \rho_P \int_{V_P} \phi_j(x)^2 \, dV_P$
j[th] beam equivalent stiffness	$K_{Bj} = c_B \int_{V_B} y^2 \phi_j''(x)^2 \, dV_B$
j[th] short-circuit piezoelements equivalent stiffness	$K_{Pj}^E = c_P^E \int_{V_P} y^2 \phi_j''(x)^2 \, dV_P$
j[th] macroscopic piezoelectric coefficient	$\alpha_j = e \int_{V_P} \dfrac{\lvert y \rvert}{e_P} \phi_j''(x) dV_P$
j[th] force coefficient	$\beta_j = \phi_j(x_F)$
Piezoelements clamped capacitance	$C_0 = 2\dfrac{\varepsilon_S L_P b}{e_P}$
Derived parameters	
j[th] open-circuit piezoelements equivalent stiffness	$K_{Pj}^D = c_P^D \int_{V_P} y^2 \phi_j''(x)^2 \, dV_P = K_{Pj}^E + \dfrac{\alpha_j^2}{C_0}$
j[th] short-circuit resonance frequency	$\omega_j^E = \sqrt{\dfrac{K_{Sj} + K_{Pj}^E}{M_{Sj} + M_{Pj}}}$
j[th] open-circuit resonance frequency	$\omega_j^D = \sqrt{\dfrac{K_{Sj} + K_{Pj}^D}{M_{Sj} + M_{Pj}}}$
j[th] squared coupling coefficient	$k_j^2 = \dfrac{\left(\omega_j^D\right)^2 - \left(\omega_j^E\right)^2}{\left(\omega_j^D\right)^2} = \dfrac{\alpha_j^2}{\left(K_{Sj} + K_{Pj}^D\right)C_0}$
j[th] equivalent damper	$C_j = \dfrac{\sqrt{\left(K_{Sj} + K_{Pj}^D\right)\left(M_{Sj} + M_{Pj}\right)}}{Q_{mj}}$

A cantilever beam with piezoelectric elements can then be modeled by the sum of mechanical oscillators corresponding to each resonance frequency of the structure. The displacement of the dynamic mass of the j[th] oscillator is r_j. Without piezoelectric elements, the motion of the different mechanical oscillators would be perfectly independent and unique functions of the driving force. It is the electromechanical properties of the piezoelectric elements which links the motion of the different mechanical oscillators to the voltage. It is here pointed out that a nonlinear processing of the piezovoltage may affect all modes of the structure.

Table 3: Variables of the model

Piezoelements voltage	V
Piezoelements outgoing current	I
j[th] displacement temporal coordinate	r_j

II. CONTROL LAWS

A. Energetic Analysis

It is considered that an electrical circuit is connected to the piezoelectric elements. This device is designed to have a damping effect on the structure. The global energy equation (8) is the summation of the N energy equation associated to each mode by multiplying both sides of (6) by the velocity and integrating over the time variable. The provided energy E_P is divided into the mechanical energy E_M (kinetic + elastic), the viscous losses E_V, and the transferred energy E_S which corresponds to the part of mechanical energy which is converted into electrical energy. These energies are summarized in Table 4.

Multiplying both terms of (7) by the voltage and integrating over the time variable show that the transferred energy is the sum of the electrostatic energy stored on the piezoelectric disk and the energy absorbed by the connected electrical device. The electrical output power can then be considered as losses when VI is positive. In the case of vibration damping, the electrical device connected to the piezoelectric elements is then designed to maximize its own consumption. A new energetic equation can then be given, expressing the provided energy as the sum of the kinetic energy E_{kin}, the potential energy E_{pot} (electrostatic + elastic) and the dissipated energy E_D (viscous losses + energy consumed in the electrical device). These energies are detailed in Table 5.

$$E_F = E_M + E_V + E_S \quad (8)$$

$$E_F = E_{pot} + E_{kin} + E_D \quad (9)$$

Table 4: Energetic terms #1

Provided energy	$E_F = \sum_{j=1}^{N} \beta_j \int_0^t F\dot{r}_j dt$
Mechanical energy	$E_M = \frac{1}{2}\sum_{j=1}^{N}\left(M_{Sj} + M_{Pj}\right)\dot{r}_j^2 + \frac{1}{2}\sum_{j=1}^{N}\left(K_{Sj} + K_{Pj}^E\right)r_j^2$
Viscous losses	$E_V = \sum_{j=1}^{N} C_j \int_0^t \dot{r}_j^2 dt$
Extracted energy	$E_S = \sum_{j=1}^{N} \alpha_j \int_0^t \dot{r}_j V dt = \frac{1}{2}C_0 V^2 + \int_0^t VI dt$

Table 5: Energetic terms #2

Kinetic energy	$E_{kin} = \frac{1}{2}\sum_{j=1}^{N}\left(M_{Sj} + M_{Pj}\right)\dot{r}_j^2$
Potential energy	$E_{pot} = \frac{1}{2}\sum_{j=1}^{N}\left(K_{Sj} + K_{Pj}^{E}\right)r_j^2 + \frac{1}{2}C_0V^2$
Dissipated energy	$E_D = \sum_{j=1}^{N} C_j \int_0^t \dot{r}_j^2 dt + \int_0^t VIdt$

B. SSDI Basis

This paper deals with a particular non linear technique which is known as SSDI for Synchronized Switch Damping on Inductor [6, 7, 8]. This nonlinear damping technique consists of adding a switching device in parallel with the piezoelectric elements. It allows to briefly reverse the piezovoltage at selected instants. This device is composed of a switch and an inductance L_I connected in series. The switch is almost always open. It is briefly closed at selected instants The capacitance C_0 of the piezoelectric elements and the inductance L_I constitute then an oscillator. The switch is kept closed until the voltage V on the piezoelectric elements has been reversed. It corresponds to a time t_i equal to a semi pseudo-period of the electric oscillator, as shown in (10). The lower the inductance L_I, the shorter will be t_i. Thus, this technique doesn't require a high inductance value. Practically, the inductance is chosen to get an inversion time roughly between twenty and fifty times lower than the shortest mechanical vibration period.

$$t_i = \pi\sqrt{L_I C_0} \tag{10}$$

When the switch is open and if no load is connected, the outgoing piezo current is null and then the voltage and the displacement vary proportionally. The voltage and displacement typical waveforms are shown in Fig. 2 in the case of a sinusoidal solicitation and when the voltage inversion instants correspond to the displacement extrema. The voltage inversion is detailed in Fig. 3.

The voltage inversion is not perfect, because a part of the energy stored on the piezoelectric elements capacitance is lost in the switching network (electronic switch+inductance). These losses are modeled by an electrical quality factor Q_I. The relation between Q_I and the voltage of the piezoelectric element before and after the inversion process is given by (11). Due to this nonlinear process, a voltage magnification is obtained and a phase shift appears between the displacement and the voltage which leads to an optimization of the extracted energy. It was shown 6 that processing the voltage on each of its extremum was optimal in the case of sinusoidal mono-modal solicitation and leads to a drastic damping effect.

$$V_{(after)} = -\gamma V_{(before)} = -V_{(before)}e^{\frac{-\pi}{2Q_I}} \tag{11}$$

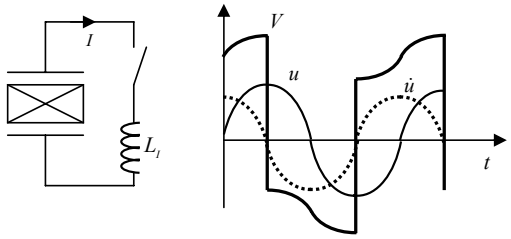

Fig. 2: SSDI device and voltage and displacement typical waveforms for a sinusoidal solicitation

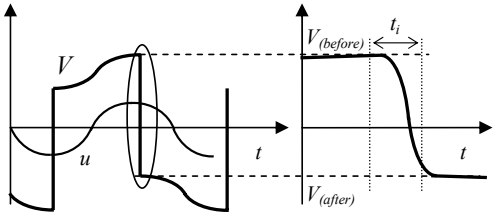

Fig. 3: Piezoelement voltage inversion

C. Multi-modal probabilistic control law

The approach proposed in this paper consists in optimizing the energy dissipated in the switching device without taking into account any information related to the different modes of the structure.

The consumption of the switching device is always zero except during the voltage inversion where it is equal to the difference of the electrostatic energy on the piezoelectric elements before and after the inversion process. The energy dissipated in the switching device is then given by (12), where V_k is the piezovoltage just before the k^{th} inversion. It appears then that maximizing the consumption of the switching device corresponds to maximizing the sum of the squared piezovoltage before each inversion.

$$\int_0^t VIdt = \frac{1}{2}C_0\sum_k V_k^2\left(1-\gamma\right) \tag{12}$$

The probabilistic approach is based on the idea of letting the voltage reach a significant but statistically probable value v_{min} before processing the voltage inversion. Since the time derivative of the extracted energy is null when the time derivative of the strain in the piezoelectric element is null, the extracted energy reaches a local extremum at each extremum of the strain in the piezoelements. Since strain and voltage extrema occurs at the same time, the piezovoltage inversion is achieved when $V^2 > v_{\min}^2$ and V^2 reaches an extremum.

The evolution of the piezovoltage between two inversion processes is given by (13), where t_k and t_{k+1} are two consecutive inversion times, $-\gamma V_k$ is the voltage after the first voltage inversion and r_{jk} is the j^{th} temporal coordinate of the displacement at instant t_k.

$$\text{for } t \in]t_k, t_{k+1}] \quad V(t) = -\gamma V_k + \frac{1}{C_0}\sum_{j=1}^{N}\alpha_j\left(r_j(t) - r_{jk}\right) \tag{13}$$

After the k^{th} inversion time, V can be considered as a continuous random function, whose cumulative distribution function is defined by (14). $v_{\min}$ is defined after each voltage

inversion so that the probability of observing $V^2 > v_{\min}^2$ is equal to P_{SW}, where P_{SW} is an arbitrary fixed probability. This is summarized in (15), where it is pointed out that $v_{\min}$ can be determining using the cumulative distribution function. Fig. 4 gives a graphical representation of (15).

$$F_{V^2}\left(v^2\right) = P\left[V^2 \le v^2\right] \tag{14}$$

$$P\left[V^2 > v_{\min}^2\right] = P_{SW} = 1 - F_{V^2}\left(v_{\min}^2\right) \tag{15}$$

The critical point of this approach consists in estimating the cumulative distribution function of the voltage after each inversion. It is then easy to determine $v_{\min}$. The evolution of the piezovoltage after the k^{th} inversion time can be estimated using (16). It is assumed that the strain in the piezoelectric elements after the switch will be similar to the strain in the piezoelectric elements before the switch. The estimation is made considering an arbitrary observation time T_{es} of the strain. This procedure is illustrated in Fig. 5.

It is then assumed that the cumulative distribution function of the piezovoltage after the k^{th} inversion time is almost equal to the one of the estimated piezovoltage. This function can be derived from the estimated piezovoltage as shown by (17) where $t_{V_{es}^2 \le v_{es}^2}$ is the cumulative time where $V_{es}^2 \le v_{es}^2$.

Practically, the estimation of the piezovoltage can be made using an open-circuited additional piezoelement bonded in the same area than the piezoelements used for the vibration control. This piezoelement is used as a strain sensor. Its voltage Vs is given by (18). Using a T_{es} recording of this voltage before the k^{th} inversion, the estimated piezovoltage can be estimated using (19) where V_{Sk} is the voltage on the sensor at the instant t_k. It is clear that (19) is strictly equivalent to (16), thus this technique can be easily implemented and does not required any filtering device.

$$V_{es}\left(t^+\right) = -\gamma V_k + \frac{1}{C_0}\sum_{j=1}^{N}\alpha_j\left(r_j\left(t^-\right) - r_{jk}\right) \quad \text{with} \begin{cases} t^+ \in \left[t_k, t_k + T_{es}\right] \\ t^- \in \left[t_k - T_{es}, t_k\right] \end{cases} \tag{16}$$

$$F_{V^2}\left(v^2\right) \approx F_{V_{es}^2}\left(v_{es}^2\right) = P\left[V_{es}^2 \le v_{es}^2\right] = \frac{t_{V_{es}^2 \le v_{es}^2}}{T_{es}} \tag{17}$$

$$V_s = \frac{1}{C_0}\sum_{j=1}^{N}\alpha_j r_j \tag{18}$$

$$V_{es}\left(t^+\right) = -\gamma V_k + V_S\left(t^-\right) - V_{Sk} \tag{19}$$

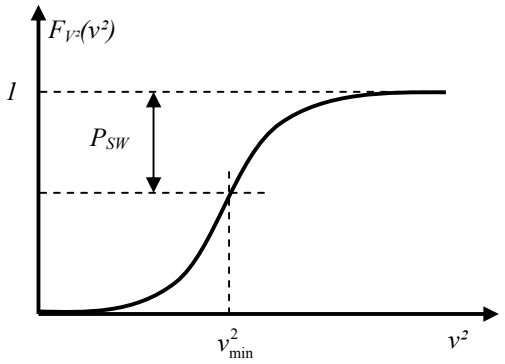

Fig. 4: Determination of v_{min}

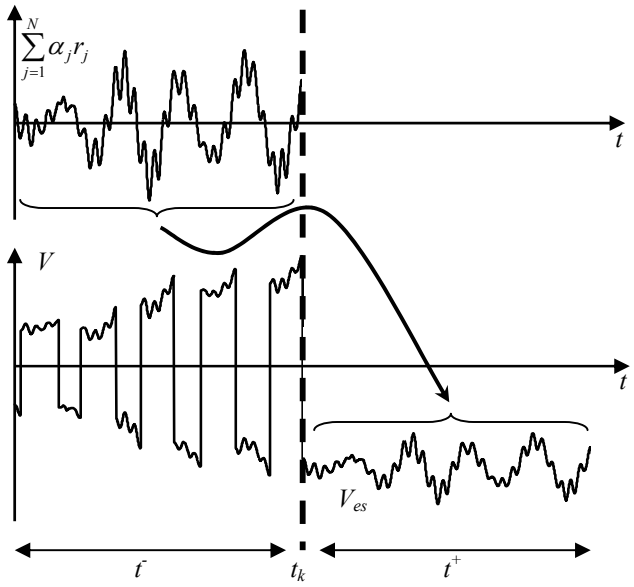

Fig. 5: Estimation of the piezovoltage after an inversion process

D. Mono-modal case

In the case of a mono-modal solicitation and providing that P_{SW}>0, the probabilistic approach basically leads to reverse the voltage at each displacement extremum, i.e. at each voltage extremum. This is illustrated in Fig. 6. The new probabilistic control law described in this paper appears then to be a generalization of the original SSDI control law which consists in reversing the voltage on each voltage extremum 6, 7, 8.

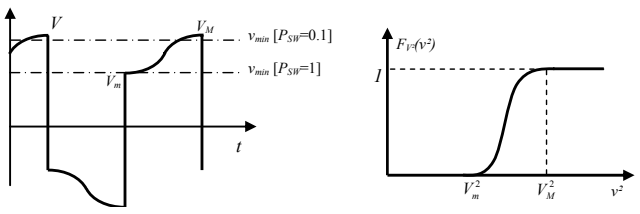

Fig. 6: Probabilistic approach in the case of a mono-modal solicitation

III. SIMULATIONS RESULTS

In this section the probabilistic approach is applied on a three modes model of a cantilever beam with piezoelectric patches and compared to the multi-modal law by mode selection. Simulations derived from numerical time domain integrations of (6) and (7). Calculations are made using a fourth order Runge Kutta algorithm with a constant integration time step.

A. Characteristics of the model used for simulations

The model corresponds to a realistic steel beam with piezoelectric elements bonded on its surface driven by a force applied at its free end. Piezoelectric patches are modeled using P189 PZT ceramics characteristics. The first three bending modes are considered. The main characteristics of this structure are summarized in

Table 6. The first three bending resonance frequencies as well as the corresponding coupling coefficients and mode shapes (plotted in Fig. 7) were determinate using a FEM simulation of the structure. The parameters of the model can be deduced from these characteristics. They are detailed in Table 7. In fact, a three dimensional FEM simulation gives two other modes, at 240 Hz and 770 Hz but these resonance frequencies do not correspond to bending modes but twist modes for which the coupling coefficient is zero because of the piezoelectric patches location. Moreover these modes can't be theoretically excited by a driving force centered along the *z* axis, that why they are not considered in this model.

Table 6: Characteristics of the structure

Beam material	steel
Beam dimension	180x90x2 mm^3
Piezoelements material	P189
Number of piezoelements	2
Piezoelement dimension	40x90x0.3 mm^3
Piezoelements position	5 mm from clamped end
Piezoelements clamped capacitance C_0	74.9 nF
Inversion quality factor Q_I	5
Resonance frequencies	56.4 Hz, 353 Hz, 990 Hz
Squared coupling coefficients	0.0092, 0.0044, 0.0007
Mechanical quality factors	400, 400, 400

Table 7: Parameters of the model

	1st Mode	2nd Mode	3rd Mode
$M_{Sj} + M_{Pj}$ (g)	62.0	62.0	62.0
$K_{Sj} + K_{Pj}^E$ (Nm^{-1})	771	30 500	2 400 000
C_j (Nm^{-1}s^{-1})	0.0549	0.344	0.964
α_j (NV^{-1})	0.00230	0.0100	0.0111
β_j	1	1	1

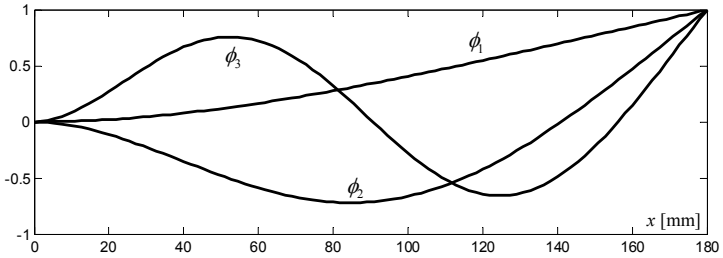

Fig. 7: Mode shapes of the structure

B. Evaluation of the vibration control effectiveness

The effectiveness of the different vibration control laws will be evaluated using two criteria. The first one is related to the displacement of the structure. It is considered the integral I_u of the squared displacement along the *x* axis and over the time. This double integral is equal to the sum of the integral over the time of the squared displacement temporal coordinate r_j, as shown in (20). The ratio of this double integral in the controlled case and in the uncontrolled case is defined as the 'displacement damping' A_u (21). The displacement damping in dB is given by (22).

$$I_u = \int_0^t \int_0^L u(x,t)^2 \, dx dt = \sum_{j=1}^{N} \int_0^t r_j(t)^2 \, dt \tag{20}$$

$$A_u = \frac{(I_u)_{controlled}}{(I_u)_{uncontrolled}} \tag{21}$$

$$A_{udB} = 10\log(A_u) \tag{22}$$

The second criterion is based on the mechanical energy of the structure. It is considered the integral I_E of the structure mechanical energy over the time (23). The 'energy damping' is defined as the ratio of this integral in the controlled case and in the uncontrolled case (24). Its expression in dB is given by (25)

$$I_E = \frac{1}{2} \sum_{j=1}^{N} \left[\left(M_{Sj} + M_{Pj} \right) \int_0^t \dot{r}_j^2 dt + + \left(K_{Sj} + K_{Pj}^E \right) \int_0^t r_j^2 dt \right] \tag{23}$$

$$A_E = \frac{(I_E)_{controlled}}{(I_E)_{uncontrolled}} \tag{24}$$

$$A_{EdB} = 10\log(A_E) \tag{25}$$

C. Simulations for a pulsed solicitation

In this section, it is considered a pulsed solicitation applied at the free end of the beam. Simulations are achieved using both the probabilistic law and the original law consisting in reversing the voltage at each extremum. Calculations are performed for 20 periods of the first resonance frequency. The fixed integration time step is chosen so that there is 50 time steps per periods of the higher (the third) resonance frequency. In the case of the probabilistic law, Simulations are performed using a strain observation time T_{es} equal to twice the period corresponding to the lower resonance frequency of the

structure. This time must be large enough to get a realistic image of the strain but must also be short enough to allow the technique to be sufficiently reactive. It appears that twice the period of the lower resonance frequency is the best compromise, but taking T_{es} anywhere between one and three times this period leads to satisfactory results.

Fig. 8 shows the displacement and energy damping in dB using the probabilistic control law as a function of P_{SW}. When P_{SW} is zero, both damping are zero because $v_{\min}$ is chosen so that the probability of observing V higher than $v_{\min}$ is zero. P_{SW}=0 corresponds then to the uncontrolled case. When P_{SW}=1 $v_{\min}$ is chosen so that the probability of observing V higher than $v_{\min}$ is one which leads to process the voltage on each strain extrema. It is shown that for an optimal value of P_{SW} equal to 0.1 the displacement and energy damping are optimized. The displacement damping reaches -7.7dB and the energy damping -6.5dB whereas it is -3.8dB and -4.8dB respectively when reversing the voltage on each strain extrema.

Fig. 9 shows the modal repartition of the mechanical energy without control, reversing the voltage on each extremum and using the probabilistic approach. The bottom patch represents the mechanical energy related to the first mode, the middle patch to the second mode and the top patch to the third mode. It is shown that the probabilistic approach allows to control all modes simultaneously whereas reversing the voltage on each extremum principally address the higher modes.

Fig. 10 shows the normalized strain in the piezoelements and the piezovoltage versus time for the different control laws.

Fig. 11 shows the corresponding displacement of the beam free end. Simulations show that both energy and displacement damping benefits from the probabilistic approach, main results in dB are summarized in Table 8.

Table 8: Simulation results for a pulsed solicitation

Control Law	A_{EdB}	A_{udB}
Switch on each extremum	-4.89	-3.81
Probabilistic – P_{SW}=0.1	-6.50	-7.67

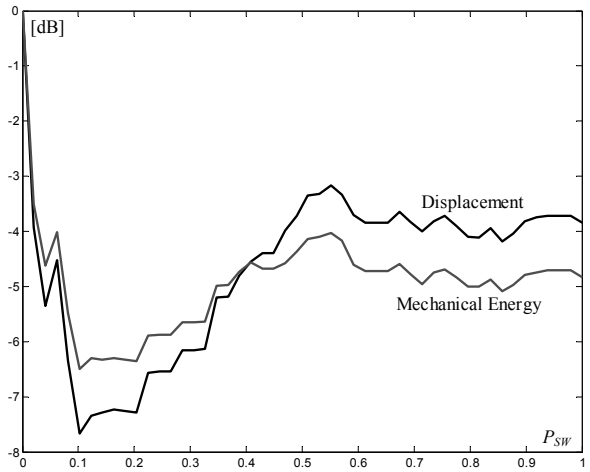

Fig. 8: Pulsed solicitation – Displacement and energy damping with the probabilistic law as a function of P_{SW}

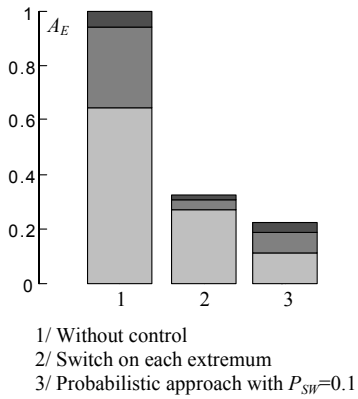

Fig. 9: Pulsed solicitation – Energy damping

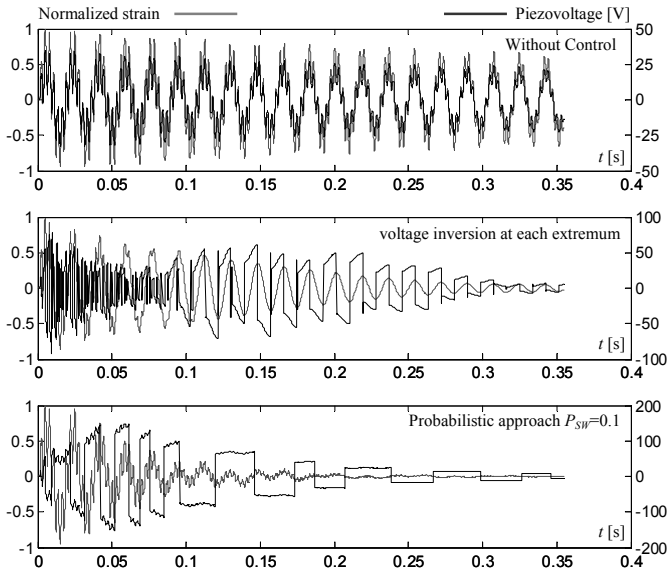

Fig. 10: Pulsed solicitation – Normalized strain and piezovoltage for different control laws

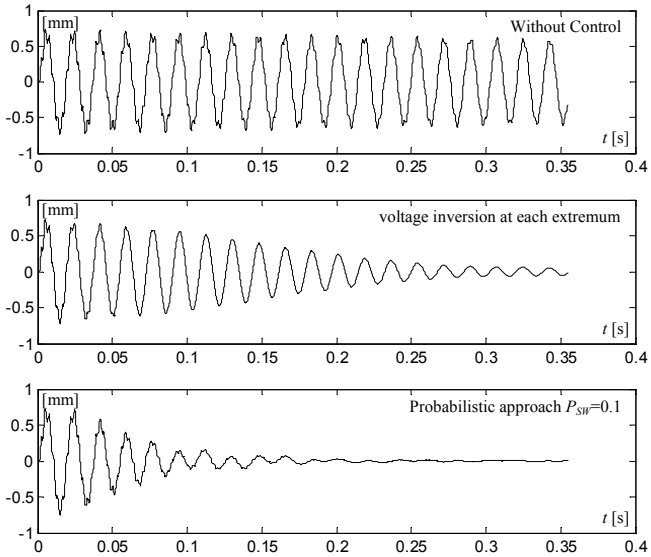

Fig. 11: Pulsed solicitation – Displacement of the beam free end for different control laws

D. *Simulations for a white noise solicitation*

In this section, a white noise solicitation is applied at the free end of the beam. The same simulations are achieved as in the previous section. Calculations are performed for 200 periods of the first resonance frequency, with the same time steps as previously.

Fig. 12 to Fig. 15 show the same results than in the previous section. Using the probabilistic approach, it is shown in Fig. 12 that the displacement and energy damping are optimized for almost the same value of P_{SW}. The optimized displacement and energy damping are -8.5dB and -6.3dB whereas it is -3.0dB and -4.3dB respectively when switching on all voltage extrema.

Fig. 13 shows that the probabilistic approach allows to control each of the three considered modes. Reversing the voltage on each extremum is not very effective to address the first mode of the structure since the extremum occurrence frequency and then the resulting switching frequency roughly corresponds to the second or the third modes.

The normalized strain and the piezovoltage as well as the displacement of the beam free end are plotted in Fig. 14 and Fig. 15 respectively. These figures are plotted for the different control laws. Only a small part of the whole simulated time is represented on these plots. Main results in dB are summarized in Table 9.

Table 9: Simulation results for a white noise solicitation

Control Law	A_{EdB}	A_{udB}
Switch on each extremum	-4.27	-2.96
Probabilistic – P_{SW}=0.1	-6.32	-8.49

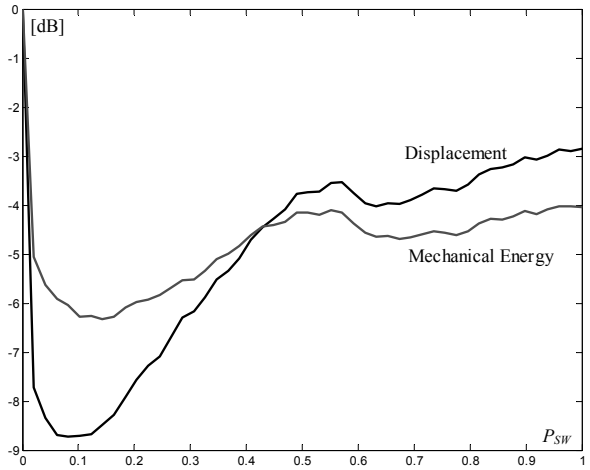

Fig. 12: White noise solicitation – Displacement and energy damping with the probabilistic law as a function of P_{SW}

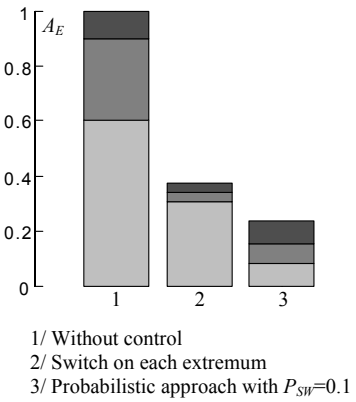

Fig. 13: White noise solicitation – Energy damping

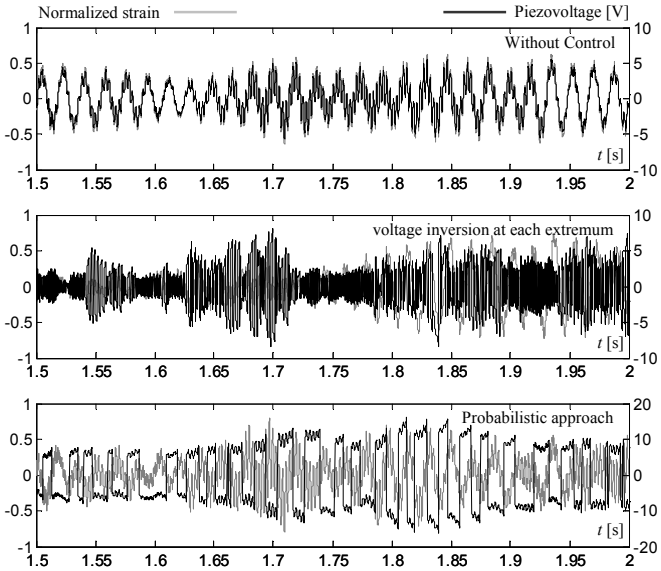

Fig. 14: White noise solicitation – Normalized strain and piezovoltage for different control laws

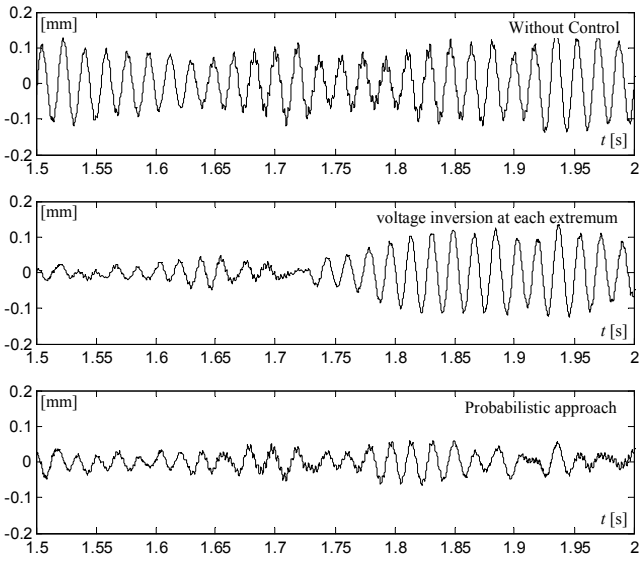

Fig. 15: White noise solicitation – Displacement of the beam free end for different control laws

CONCLUSION

The novel multi-modal probabilistic approach described in this paper is dedicated to the SSDI technique. It was shown that this control law allows to simultaneously optimize both displacement based and energy based vibration control criteria. It is much more effective than the original control law consisting in processing the piezovoltage on each strain extrema. The probabilistic control law may also be very easily implemented, since it does not require any filtering device nor any information related to the modes of the structure. The only required information is the piezovoltage itself and the strain in the piezoelements which can be deduced from an additional piezoelement used as sensor or from the processed voltage itself.

Many industrial sectors could benefit from this technique. It has the advantage of its simplicity and of its very low power requirements, since contrary to active control techniques no power amplifiers are required.

Current work consists in implementing this technique on a digital signal processor (DSP) and testing it on a real experimental set-up.

REFERENCES

1. Hagood N W & Von Flotow A, 'Damping of structural vibrations with piezoelectric material and passive electrical networks', Journal of Sound and Vibration, Vol. 146, p243, 1991
2. Wu S, "Method for multiple shunt damping of structural vibration using a single PZT transducer", Proc. SPIE SSMat. Conf., Passive Damping and Isolation, San Diego, 1998, vol 3327, p159, 1998.
3. C L Davis & G A Lesieutre, "An actively tuned solid-state vibration absorber using capacitive shunting of piezoelectric stiffness", Journal of Sound and Vibration, Vol. 232, pp. 601-617, 2000.
4. R A Morgan & K W Wang, "Active-passive piezoelectric absorbers for systems under multiple non-stationary harmonic excitations", Journal of Sound and Vibration, Vol. 255(4), pp. 685-700, 2002
5. W W Clark, "Vibration control with state-switching piezoelectric material", J. Intell. Mater. Syst. Struct., Vol.11, p 263, 2000.
6. C Richard, D Guyomar D Audigier & G Ching, "Semi passive damping using continuous switching of a piezoelectric device", Proc. SPIE SSMat. Conf., Passive Damping and Isolation, San Diego, vol 3672, p104, 1998.
7. C Richard, D Guyomar D Audigier & H Bassaler, "Enhanced semi passive damping using continuous switching of a piezoelectric device on an inductor", Proc. SPIE SSMat. Conf., Passive Damping and Isolation, vol 3989, p288, 2000.
8. D Guyomar, C Richard & L. Petit, "Non-linear system for vibration damping", proc. 142th ASA Meeting, St Lauderdale, 2001.
9. L. R. Corr, W. W. Clark, "A Novel Semi-Active Multi-Modal Vibration Control Law for a Piezoceramic Actuator", Transactions of the ASME, vol. 125, pp. 214-222, April 2003
10. H. A. Sodano, G. Park, D. J. Inman, "Estimation of Electrical Charge Output for Piezoelectric Energy Harvesting", Strain, vol. 40, pp. 49-58, 2004